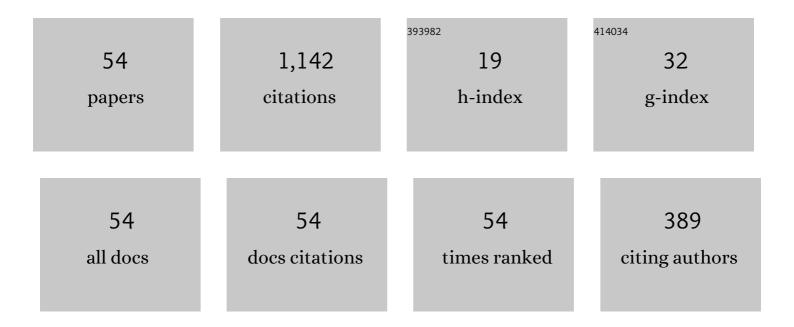
## Alaa F Abd El-Rehim

List of Publications by Year in descending order

Source: https://exaly.com/author-pdf/6783846/publications.pdf Version: 2024-02-01



#	Article	IF	CITATIONS
1	Physical, Radiation Shielding and Crystallization Properties of Na2O-Bi2O3- MoO3-B2O3- SiO2-Fe2O3 Glasses. Silicon, 2022, 14, 405-418.	1.8	46
2	Optical Properties of SiO2 – TiO2 – La2O3 – Na2O – Y2O3 Glasses and A Novel Process of Preparing the Parent Glass-Ceramics. Silicon, 2022, 14, 373-384.	1.8	32
3	Nanomaterial-based biosensors for COVID-19 detection. Critical Reviews in Solid State and Materials Sciences, 2022, 47, 955-978.	6.8	5
4	FT-IR and Gamma Shielding Characteristics of 22SiO2- 23Bi2O3-37B2O3-13TiO2-(5-x) LiF- x BaO Glasses. Silicon, 2022, 14, 7043-7051.	1.8	40
5	Exchange bias and magnetocrystalline anisotropy of non-stoichiometric CoxFe3â^'xO4 nanoparticles. Journal of Materials Science: Materials in Electronics, 2022, 33, 9629-9640.	1.1	2
6	Characterization of Ultramafic–Alkaline–Carbonatite complex for radiation shielding competencies: An experimental and Monte Carlo study with lithological mapping. Ore Geology Reviews, 2022, 142, 104735.	1.1	29
7	Camma Radiation Shielding and Mechanical Studies on Highly Dense Lithium Iron Borosilicate Glasses Modified by Zinc Oxide. Silicon, 2022, 14, 10391-10399.	1.8	19
8	Structural, elastic, electronic and optical properties of the newly synthesized selenides Tl2CdXSe4 (X = Ge, Sn). European Physical Journal B, 2022, 95, 1.	0.6	6
9	Fabrication of lithium borosilicate glasses containing Fe2O3 and ZnO for FT-IR, UV–Vis–NIR, DTA, and highly efficient shield. Applied Physics A: Materials Science and Processing, 2022, 128, 1.	1.1	22
10	Physical, Optical, and Radiation Shielding Features of Yttrium Lithium Borate Glasses. Journal of Inorganic and Organometallic Polymers and Materials, 2022, 32, 2873-2881.	1.9	24
11	Optical investigations of Cu2CdSnS <mml:math <br="" xmlns:mml="http://www.w3.org/1998/Math/MathML">display="inline" id="d1e335" altimg="si2.svg"&gt;<mml:msub><mml:mrow /&gt;<mml:mrow><mml:mn>4</mml:mn></mml:mrow></mml:mrow </mml:msub></mml:math> quaternary alloy nanostructure for indoor optical wireless communications. Optics Communications. 2022, 517, 128351.	1.0	1
12	Effect of Fe2O3 as an Aggregate Replacement on Mechanical, and Gamma/ Neutron Radiation Shielding Properties of Phosphoaluminate Glasses. Journal of Inorganic and Organometallic Polymers and Materials, 2022, 32, 3117-3127.	1.9	23
13	Investigation of the Structural, Elastic, Electronic, and Optical Properties of Half-Heusler CaMgZ (Z =) Tj ETQq1 1 (	0.784314 1.0	rgBT /Overlo
14	Investigation of structural, magneto-electronic, elastic, mechanical and thermoelectric properties of novel lead-free halide double perovskite Cs2AgFeCl6: First-principles calcuations. Journal of Physics and Chemistry of Solids, 2022, 167, 110795.	1.9	108
15	Effect of Strain on the Electronic Structure and Phonon Stability of SrBaSn Half Heusler Alloy. Molecules, 2022, 27, 3785.	1.7	3
16	Radiation, Crystallization, and Physical Properties of Cadmium Borate Glasses. Silicon, 2021, 13, 2289-2307.	1.8	48
17	Spectroscopic, Structural, Thermal, and Mechanical Properties of B2O3-CeO2-PbO2 Glasses. Journal of Inorganic and Organometallic Polymers and Materials, 2021, 31, 1774-1786.	1.9	51
18	Structural and Mechanical Properties of Lithium Bismuth Borate Glasses Containing Molybdenum (LBBM) Together with their Glass–Ceramics. Journal of Inorganic and Organometallic Polymers and Materials, 2021, 31, 1057-1065.	1.9	52

#	Article	IF	CITATIONS
19	Influence of Sb <sub>2</sub> O <sub>3</sub> Nanoparticles Addition on the Thermal, Microstructural and Creep Properties of Hypoeutectic Sn–Bi Solder Alloy. Science of Advanced Materials, 2021, 13, 20-29.	0.1	2
20	Mathematical Modelling of Vickers Hardness of Sn-9Zn-Cu Solder Alloys Using an Artificial Neural Network. Metals and Materials International, 2021, 27, 4084-4096.	1.8	13
21	Influence of La2O3 content on the structural, mechanical, and radiation-shielding properties of sodium fluoro lead barium borate glasses. Journal of Materials Science: Materials in Electronics, 2021, 32, 4651-4671.	1.1	55
22	Structural, Elastic Moduli, and Radiation Shielding of SiO2-TiO2-La2O3-Na2O Glasses Containing Y2O3. Journal of Materials Engineering and Performance, 2021, 30, 1872-1884.	1.2	54
23	Effect of Bi Content on the Microstructure and Mechanical Performance of Sn-1Ag-0.5Cu Solder Alloy. Crystals, 2021, 11, 314.	1.0	4
24	Modelling the Effect of Cu Content on the Microstructure and Vickers Microhardness of Sn-9Zn Binary Eutectic Alloy Using an Artificial Neural Network. Crystals, 2021, 11, 481.	1.0	9
25	Dispersion Parameters, Polarizability, and Basicity of Lithium Phosphate Glasses. Journal of Electronic Materials, 2021, 50, 3116-3128.	1.0	43
26	The joint effect of naphthalene-system and defects on dye removal by UiO-66 derivatives. Microporous and Mesoporous Materials, 2021, 325, 111314.	2.2	16
27	Advanced nuclear radiation shielding studies of some mafic and ultramafic complexes with lithological mapping. Radiation Physics and Chemistry, 2021, 189, 109777.	1.4	27
28	Morphological and optical investigations of the NiZnFe2O3 quaternary alloy nanostructures for potential application in optoelectronics. Journal of Taibah University for Science, 2021, 15, 275-281.	1.1	4
29	MW synthesis of ZIF-65 with a hierarchical porous structure. Microporous and Mesoporous Materials, 2020, 293, 109685.	2.2	15
30	The effects of La2O3 addition on mechanical and nuclear shielding properties for zinc borate glasses using Monte Carlo simulation. Ceramics International, 2020, 46, 29191-29198.	2.3	75
31	Enhanced room temperature ammonia gas sensing properties of Al-doped ZnO nanostructured thin films. Optical and Quantum Electronics, 2020, 52, 1.	1.5	13
32	Structural characterization and optical properties of zeolitic imidazolate frameworks (ZIF-8) for solid-state electronics applications. Optical Materials, 2020, 100, 109648.	1.7	31
33	Simulation and Prediction of the Vickers Hardness of AZ91 Magnesium Alloy Using Artificial Neural Network Model. Crystals, 2020, 10, 290.	1.0	13
34	Modification of ZIF-8 with triethylamine molecules for enhanced iodine and bromine adsorption. Inorganica Chimica Acta, 2020, 509, 119678.	1.2	17
35	Microhardness and microstructure characteristics of AZ91 magnesium alloy under different cooling rate conditions. Materials Research Express, 2019, 6, 086572.	0.8	11
36	Microstructure evolution and tensile creep behavior of Sn–0.7Cu lead-free solder reinforced with ZnO nanoparticles. Journal of Materials Science: Materials in Electronics, 2019, 30, 2213-2223.	1.1	14

#	Article	IF	CITATIONS
37	The Mechanical and Microstructural Changes of Sn-Ag-Bi Solders with Cooling Rate and Bi Content Variations. Journal of Materials Engineering and Performance, 2018, 27, 344-352.	1.2	13
38	Effect of TiO2 Nanoparticles Addition on the Thermal, Microstructural and Room-Temperature Creep Behavior of Sn-Zn Based Solder. Journal of Electronic Materials, 2018, 47, 6984-6994.	1.0	18
39	Effect of Graphitic Carbon Nitride Nanosheets Addition on the Microstructure and Mechanical Properties of Sn-3.5Ag-0.5Cu Solder Alloy. Journal of Electronic Materials, 2018, 47, 5614-5624.	1.0	8
40	Evaluation of laser Induced Breakdown Spectroscopy for analysis of annealed Aluminum Germanium alloy at different temperatures. IOP Conference Series: Materials Science and Engineering, 2018, 383, 012012.	0.3	2
41	Investigation of microstructure and mechanical properties of Sn-xCu solder alloys. Journal of Alloys and Compounds, 2017, 695, 3666-3673.	2.8	36
42	Effect of aging treatment on microstructure and creep behaviour of Sn–Ag and Sn–Ag–Bi solder alloys. Materials Science and Technology, 2014, 30, 434-438.	0.8	15
43	Influence of quenching conditions on the mechanical and structural properties of Al–30wt% Zn alloy. Materials Science & Engineering A: Structural Materials: Properties, Microstructure and Processing, 2014, 602, 105-109.	2.6	2
44	Effect of Cu addition on the microstructure and mechanical properties of Al–30wt% Zn alloy. Journal of Alloys and Compounds, 2014, 607, 157-162.	2.8	8
45	Transient and steady state creep of age-hardenable Al–5Âwt% Mg alloy during superimposed torsional oscillations. Journal of Materials Science, 2013, 48, 2659-2669.	1.7	6
46	Effect of cyclic stress reduction on high temperature creep characteristics of solid solution Alâ^'2·9 wt-Mg alloy. Materials Science and Technology, 2011, 27, 44-48.	0.8	1
47	Effect of torsional oscillations on the stress–strain behavior of Al–5wt% Mg alloy. Materials Science & Engineering A: Structural Materials: Properties, Microstructure and Processing, 2011, 528, 6026-6033.	2.6	5
48	The enhancement of creep in Al–22Âwt% Ag alloy by cyclic stressing. Journal of Materials Science, 2010, 45, 1579-1587.	1.7	3
49	The variation of work hardening characteristics of Al-5wt% Mg alloy during phase transition. Physica B: Condensed Matter, 2010, 405, 3616-3623.	1.3	10
50	Effect of superimposed oscillations on creep behaviour of Al – 2 4•.5Cu and Al – 2 4•5Cu – 2 0•1In (wt-%) alloys containingl̂,′ precipitates. Materials Science and Technology, 2007, 23, 620-626.	0.8	4
51	Examination of breakdown stress in creep by viscous glide in Al–5·5 at%Mg solid solution alloy at high stress levels. Materials Science and Technology, 2007, 23, 1144-1148.	0.8	3
52	Effect of structure transformation on the creep characteristics of Sn–3wt% Bi alloy. Journal of Alloys and Compounds, 2007, 440, 127-131.	2.8	4
53	Study of precipitates formation in Al-4.5Wt%Cu and Al-4.5Wt%Cu-0.1Wt%In alloys using creep measurements and positron annihilation technique. Crystal Research and Technology, 2005, 40, 665-671.	0.6	7
54	Plastic deformation of Al-4.5 wt% Cu and Al-4.5 wt% Cu-0.1 wt% In alloys under the effect of cyclic stress reduction. Physica Status Solidi A, 2004, 201, 2295-2304.	1.7	5